愛知工業大学研究報告
第 46 号　平成 23 年

大気圧 Ar/He マイクロ波プラズマ・ジェットの生成と消滅過程

Formation and Decay Processes of Ar/He Microwave Plasma Jet at Atmospheric Gas Pressure

高村秀一†，天野慎太†，倉田達也†，笠田裕貴†，山本潤†，アブドゥール・ラザック†，櫛田玄一郎†，
大野哲靖††，神藤正士†††
Shuichi TAKAMURA, Shinta AMANO, Tatsuya KURATA, Hirotaka KASADA, Jun YAMAMOTO,
M.Abdur RAZZAK, Genichiro KUSHIDA, Noriyasu OHNO, Masashi KANDO

Abstract　Dynamic behaviors of gas/plasma mixture produced with microwave discharge jet at atmospheric pressure have been investigated in terms of the effects of working gas dynamics on the discharge characteristics, focusing on the following four points : formation of discharge jet at the ignition phase, growing speed of plasma plume in relation to gas flow rate, acceleration and deceleration of upward movement of plasma plume, and decay process of plasma column at turn-off of microwave power.

1. Introduction

The microwave discharges at atmospheric gas pressure have been investigated and applied to many industrial purposes[1～6]. The gas flow has a general importance in fluid mechanics owing to a development of turbulence, gas mixing in diffusion flame[7], gas flow dynamics and many other applications. The plasma jet discharge in atmospheric gas pressure may contain combined characteristics: flow of working gas and electrostatic force among plasma particles. The fluid mechanical property of gas flow may influence on the discharge phenomena[8, 9], and the electrostatic collective force of plasma may produce or modify the gas flow[10]. Such a strong coupling between the plasma with electrostatic force and the gas fluid with gas flow may open an interdisciplinary new research area. From this motivations, dynamic behaviors of plasma/gas mixture, especially the effects of working gas dynamics on the discharge and plasma characteristics, are focused in the present study.

The following four topics have been investigated : (1) formation at discharge start-up for plasma jet, (2) growing speed of the plasma plume in relation to gas flow speed, (3) acceleration and deceleration of upward movement of plasma plume, and (4) decay process of plasma column at turn-off of microwave power.

2. Experimental Setup

2.1 Microwave Circuit

The microwave circuit for the frequency of 2.45 GHz with TIAGO (Torche à Injection Axiale sur Guide d'Ondes, in French) nozzle launcher with a hole of 1mm in diameter[1, 9, 11] for plasma jet at atmospheric gas pressure has been employed as shown in Figs. 1 and 2(a), associated by tapered waveguide and the short

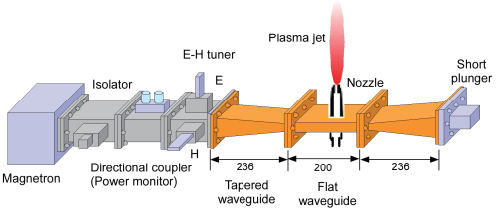

Fig.1 Experimental setup for microwave circuit.

†　Faculty of Engineering, AIT, Toyota 470-0392
††　Graduate School of Engineering, Nagoya Univ. Nagoya 464-8603
†††　Research Institute of Electronic Engineering, Shizuoka Univ. 432-8011

plunger at the end. The microwave power is less than 1 kW, and can be modulated by square wave with a time constant of less than 5 μs without any overshoot at the rising phase (Nissin Co., MG-30; MPS-30D). A high-speed imaging with a frame rate of less than 10,000 fps (FASTCAM SA-5, Photron Co.) reveals various kinds of structural dynamics. The working gas is either argon or helium.

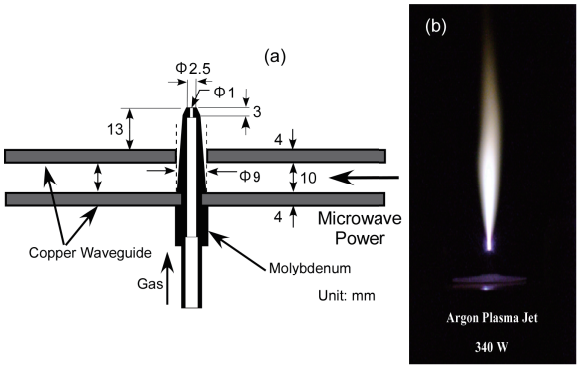

Fig.2 (a) Gas-microwave coupling structure, modified TIAGO nozzle set on the waveguide, and (b) still photo of microwave plasma jet.

The details of modified TIAGO nozzle is shown in Fig.2(a) with a typical still photo of argon plasma jet in Fig.2(b). There have been many investigations for the plasma jets produced with original as well as modified TIAGO nozzle[12~16].

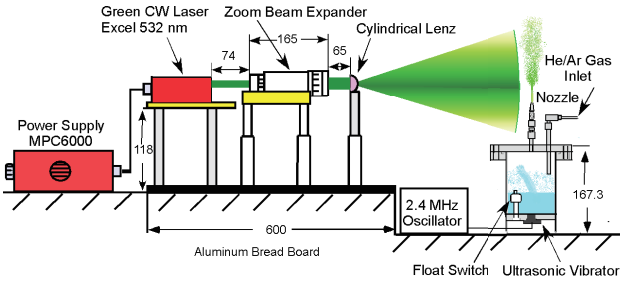

Fig.3 Laser light system for gas flow pattern visualization.

2.2 Optical System for Gas Motion Visualization

Observation of working gas motion is crucial for understanding of plasma dynamics so that the laser light system for this purpose has been prepared. A green CW laser with the maximum power of about 1 W (Excel, Quantum Ltd.) has been applied. Figure 3 shows the optics together with the modified TIAGO nozzle on the gas/mist mixing chamber. The diameter of laser light is expanded 6 times as large as that of the original laser beam, followed by a cylindrical lens to have a thin vertical fan-beam with a wide angle which irradiates the water mist effused from the nozzle with the working carrier gas of he or Ar. The diameter of nozzle is 1mm as drawn in Fig.2(a). The system is not optimized for PIV (Particle Imaging Velocimetry) since the laser sheet is too thick to have an enough spatial resolution.

3. Formation Process

First we focus on the initial stage at discharge ignition. Figure 4 gives an example of a very high-speed imaging, 10,000 fps, which is summarized for the light-emitting height of plasma plume as a function of time as shown in Fig.5(a). Four stages are identified; A: A single streamer for discharge triggering produced with the use of automobile spark plug located at the height of 20mm from the nozzle head, which is powered electronically with a FET transistor circuit, B: Transient discharge period towards an optimum length of core body. It corresponds to so called “leader” in lightning terminology which grows as becoming fat first around the streamer and then shortening its height due to the absence of discharge triggering, C: Formation and heating of core body due to the consumption of microwave power and D: Upward growth of light emitting plasma plume either by buoyancy and/or viscosity of upward moving gas flow. Figure 5(b) gives schematic pictures corresponding to the above four stages.

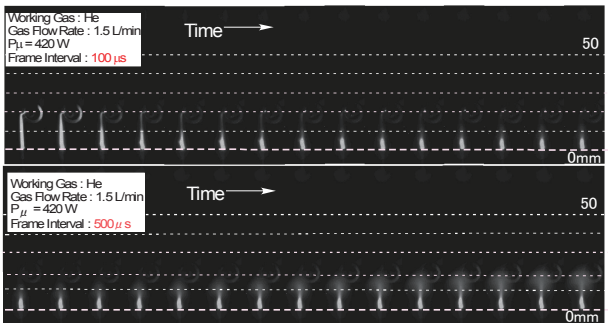

Fig.4 High-speed imaging of plasma formation at the discharge ignition. The top figure shows photos for an initial 1.4 ms with frame-to-frame interval of 100 μs, and the bottom one does those for the following 7 ms with the frame interval of 500 μs. The trigger electrode located at the center of shadowed circle is put at the height of 20 mm.

We define the vertical length of heated core body, *L*,

as shown in Fig.5(a), the intersection of plume height at t = 0, obtained by extrapolating the line showing the plasma plume as a function of time. This starting height L is plotted as a function of either microwave power or gas flow rate in Figs.6(a) and (b), respectively. We have weak increases against both the microwave power and gas flow rate, which seem reasonable.

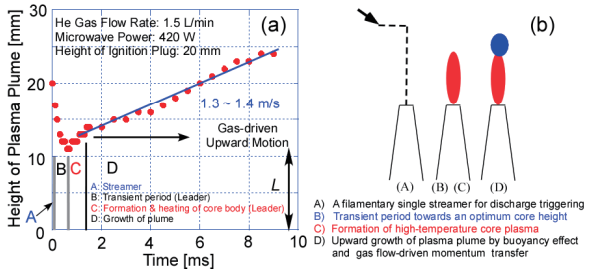

Fig.5 (a)Temporal change in height of vertical plasma column. Four formation stages are identified with (b) the possible model.

Concerning the heating stage C, a simple power balance calculation has been done as follows: A typical time scale and the input power are 1ms and 400W, respectively. It gives an injected energy of 0.4 J. If the core body has as diameter of 1cm and a length of 2 cm with the plasma density[13, 15] of $n = 10^{20}$ m^{-3}, then the internal energy of core body is roughly given by $nVe(\phi_i + 2T)$ where V is the volume of core body, ϕ_i is the ionizing potential and T is the plasma temperature in eV. It gives 0.3 J for He when T ～1 eV. These two values of energy agree approximately.

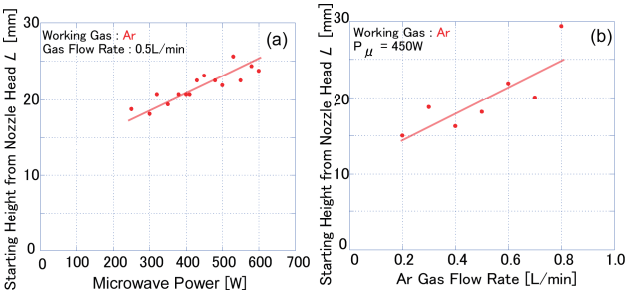

Fig.6 Dependences of initial plasma height L on (a) microwave power and (b) gas flow rate.

4. Growing Dynamics of Plasma Column

4.1 Upward Velocity of Plasma Plume

In the application of plasma jet, sometimes the time-dependent ignition may be employed. In those cases the dynamics of plasma column at the ignition and the decay would be important to know. Moreover, such behaviors are also attractive from the scientific view of collective characteristics of gas/plasma mixture medium. There have been few investigations on this subject.

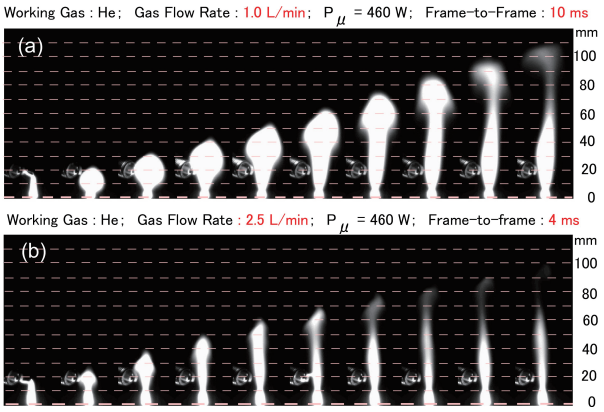

Fig.7 Upward movements of He plasma plumes for the gas flow rates of (a) 1.0 L/min and (b) 2.5 L/min.

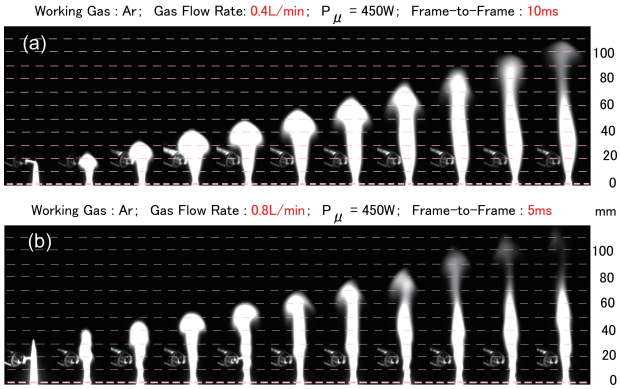

Fig.8 Upward movements of Ar plasma plumes for the gas flow rates of (a) 0.4 L/min and (b) 0.8 L/min.

Figures 7 and 8 show series of typical high-speed images of He and Ar plasma jets at the ignition. A streamer electrode is located at the height of 20 mm. Figure 9 indicates almost constant upward velocity of the upper edge of light-emitting plume, and L is the initial height of generated core plasma.

Upward velocity of He plasma plume is plotted as a function of the gas flow rate as shown in Figure 10(a) where the error bars show the velocity ranges over the whole height because the upward velocity changes in its height (see Section 4.2). The dominated upward driving force may be discriminated at about 1.0 L/min in the He case. Above this value of gas flow rate, the

upward velocity increases proportionally to the gas flow rate. It is considered as mainly gas-driven although the effect of buoyancy remains. Buoyancy-driven regime gives the velocity of around 0.5 m/s obtained at the height of 40～60 mm and at the gas flow rate of less than 1.0 L/min. A similar behavior is also observed for Ar with the discriminating gas flow rate of around 0.13 L/min which is much smaller than that for He, as shown in Fig.10(b).

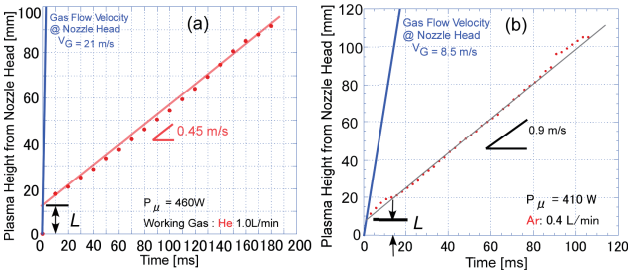

Fig.9 Top height of plasma plume for (a) He and (b) Ar as a function of time elapsed from discharge ignition. L is the intercept of straight extension line.

We note that the upward velocities of plasma plume for both He and Ar as working gases are much smaller than the gas effusing velocity V_G at the nozzle exit. However, the gas-driven velocity for Ar plasma, roughly $0.086V_G$ is about twice as large as those for He, about $0{,}048V_G$. The reason of this difference is not clear at the moment what could be related to gas viscosity although the viscosities at the room temperature for Ar and He are almost the same[17].

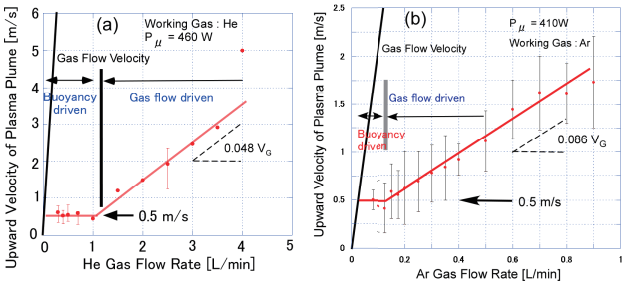

Fig.10 Dependences of upward velocities of (a) He and (b) Ar plasma plumes on each gas flow rate. The upward driving force is discriminated at about 1.0 L/min for He and about 0.13 L/min for Ar. Error bars come from the change in upward velocity on the way of growing.

Bernoulli's principle considering energy and mass conservations gives $v_2 = \sqrt{2gL^*(T_1 - T_2)/T_1}$ where g is the gravitational acceleration, 9.81 m/s^2, L^* is the so-called chimney height, and here may correspond to the initial height of core plasma column L, T_1 is the average inside temperature of plasma plume and T_2 is the outside air temperature. When T_1 is much higher than T_2, then v_2 = 0.44 or 0.63 m/s for L^* = 10 mm or 20 mm, respectively, which corresponds to L defined above as in Figs.5(a) and 9. v_2 is close to the experimental observation of 0.3～0.4 m/s at the lowest position corresponding to the buoyancy-driven starting point (see Fig.11).

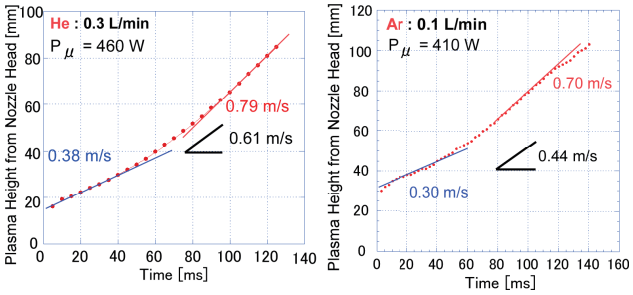

Fig.11 Acceleration of plasma plume head for (a) He and (b) Ar due to buoyancy effect.

4.2 Acceleration and Deceleration

When we examine the detail of upward movement of plasma plume, acceleration or deceleration has been observed over the upward vertical scale, depending on the gas flow speed at the nozzle head. Figure 11 gives typical examples for the acceleration in upward velocity over the height. The minimum and maximum velocities are written in these figures, while the medium velocities observed at the height of 40～60 mm are also indicated in the same figures. In the small gas flow rate like in Fig. 11, an acceleration is detected, which may occur due to the buoyancy of hot plume, while in the case of the very high flow rate like in Fig.12 a deceleration occurs, where the upward velocity is determined mainly by gas flow driven. However, the gas flow becomes turbulent starting from close to the nozzle head due to Kevin-Helmholtz instability[1, 9] which is confirmed by the visualization of gas flow pattern with mixing of water mist and carrier gas (He or Ar) as shown in Fig.13 for He and Fig.14 for Ar. The upward gas momentum diffuses toward perpendicular

to the vertical flow. Such a momentum diffusion may bring a deceleration.

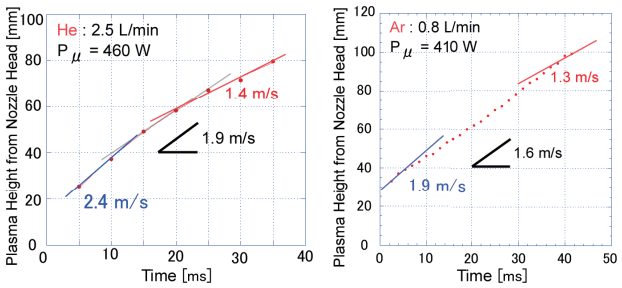

Fig.12 Deceleration of plasma plume head for (a) He and (b) Ar due to momentum diffusion with gas turbulence.

The experimental setup for the visualization of gas motion is already shown in Fig.3. The vertical height of laminar gas layer, which is detected as a green thin thread of scattered height, is plotted as a function of gas flow rate in Figs.13 and 14. In the case of He the critical gas flow rate is around 1.0 L/min below which we do not observe any turbulent behavior in the view area of laser fan beam. That for Ar is around 0.2 L/min.

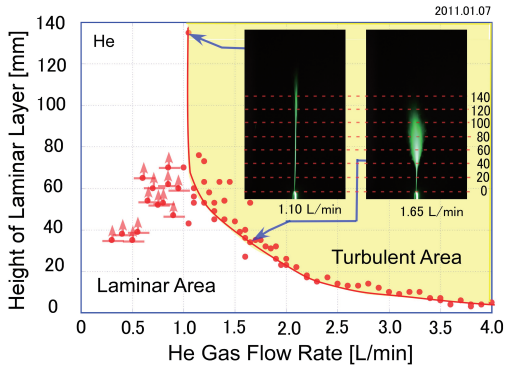

Fig.13 Boundary between laminar and turbulent zones of helium gas jet from modified TIAGO nozzle as a function of gas flow rate.

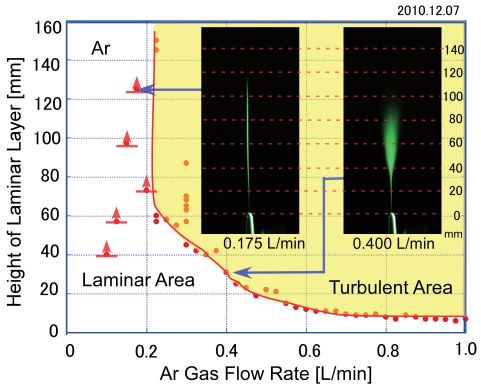

Fig.14 Boundary between laminar and turbulent zones of argon gas jet from modified TIAGO nozzle as a function of gas flow rate.

In the previous report[9], it is observed that Kelvin-Helmholtz instability start at 30 m/s (1.4 L/min) for He and 5 m/s (0.25 L/min) for Ar, corresponding to Reynolds number of 500 for He and 800 for Ar, respectively. At these gas flow rates Figs.13 and 14 give the vertical height starting turbulent flow of around 40 ～50 mm, which is roughly equal to the plasma jet height. It seems that the gas flow rate which gives a turbulent gas flow very close to nozzle head, say at 10 ～20 mm, is higher than the critical flow rate for the onset of K-H instability in plasma jet which was discussed in references (1) and (9). However, the overall tendency explains the effect of gas turbulence on the fluid dynamical instability and momentum diffusion. The difference may come from the counter effect of electrostatic force on the gas dynamics[10]. But it is not clear at the moment.

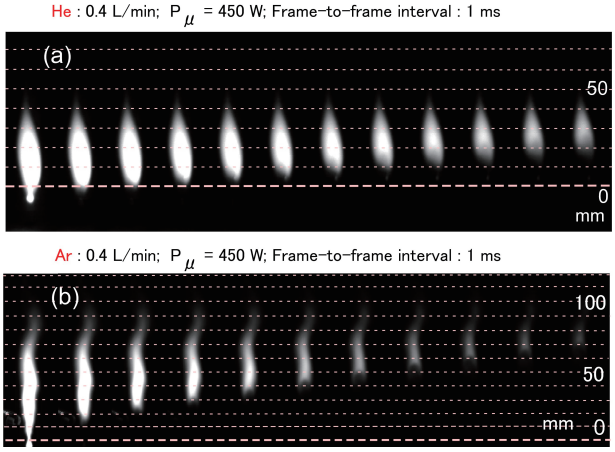

Fig.15 Decay dynamics of plasma column after turn-off of microwave power for the working gas of (a) He and (b) Ar.

5. Decay Process

The current microwave source can provide a sharp cut-off of microwave power so that dynamic behavior can be followed in time with high speed imaging. Figure 15 shows a series of photos for 10 ms after the interception of microwave power. The overall shape of helium plasma flame does not change except that the bottom becomes cut away due to the gas cooling. The height of bottom edge from the nozzle head is plotted as a function of time, as shown in Fig. 16, which gives almost a straight line with error bars, meaning a constant decay velocity. The error bars come from the shape of emitting bottom as shown in the insertion of Fig. 16. In the case of argon plasma jet, the decaying process is similar to the helium case, but we have a

much faster extinction. It is found that the plasma decay speed is much higher than the growing one, roughly by an order of magnitude. The decay speed seems to be close to the gas flow velocity. In Fig.17, they are compared with the gas flow velocity at the nozzle head, V_G. In helium plasma jet, the straight line gives $0.36V_G$ with an under off-set, while the line for Ar does $0.45V_G$ with an over off-set.

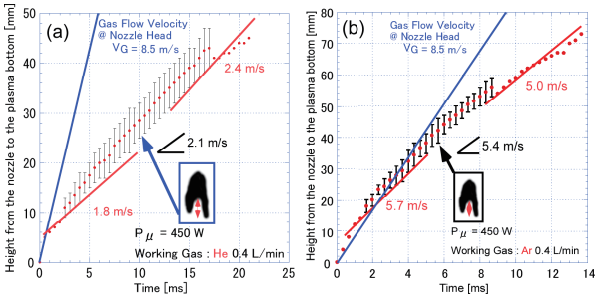

Fig.16 Bottom height of afterglow plasma column of (a) He and (b) Ar as a function of time from microwave turn-off. The error bars come from the concave shape of the plume foot.

It should be better if we can compare the local decay velocity with the local gas upward velocity. It could give a closer agreement between these two quantities, especially for Ar, which suggests the rapid decay may come from the cooling due to the contact of plasma plume with upward fresh cold gas. It takes more time to have a decay due to cooling of helium gas because the recombination rate may be lower than Ar plasma[18].

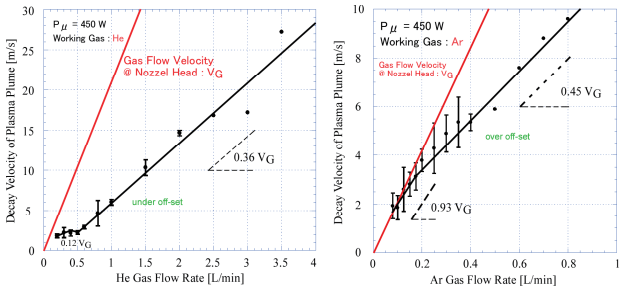

Fig.17 Dependence of plasma decay speed on (a) He and (b) Ar gas flow rate.

The decay of plume may come from the following two atomic and molecular processes leading to the quench of the electronic excitation:

(1) The electron cooling due to the inelastic as well as elastic collisions with working gas atoms or molecules.

(2) The plasma electron-ion recombinations due to radiative or three-body processes.

At the moment the physical reason for the decay process is open to be studied in future with spectroscopic method.

6. Summary and Conclusion

Strong coupling between the plasma with electrostatic force and the gas fluid with flow may open an interdisciplinary new research area. From this motivation, dynamic behaviors of plasma/gas mixture, the effect of gas motion on the plasma dynamics in particular, are focused in the present study. First, dynamic structural formation of microwave-sustained plasma jet at atmospheric gas pressure has been investigated with high speed imaging. Four stages (1)～(4) are identified at the discharge ignition as follows,

(1) Filamentary streamer formation for the discharge triggering with very short time

(2) Transient period towards the optimum core height. It develops firstly by becoming fat along the streamer and secondarily by some shortening of its length.

(3) Heating of short (L = 10～20mm) core body by consumption of microwave power

(4) Growth of plasma column due to buoyancy- and/or gas-driven upward force.

Concerning upward motions of plasma plume, the speed is discriminated by a certain gas flow rate. The two areas are identified as follows: (1) buoyancy-driven region for low flow rate and (2) gas flow driven one for high flow rate.

Acceleration or deceleration of upward movement has been found. The acceleration comes from buoyancy effect, and the deceleration does from momentum diffusion due to gas flow turbulence which was observed as a visible picture with ultrasonic water evaporator.

Decay of plasma column at power shut-off is considered to come from cooling of plasma due to fresh gas flow. The decay speed is sensitive to the local gas flow velocity which is influenced by the momentum diffusion due to gas flow turbulence, and also the recombination rate.

7. Acknowledgement

This work is performed with the support and under the auspices of the NIFS Collaboration Research

program (NIS08KOBP010) and Grant-in-Aid for JSPS Fellows (20-08409). It is also supported in part by a Grant-in-Aid for Scientific Research (B)(20360414 from JSPS).

References

1) S. Takamura, S. Saito, G. Kushida, M. Kando and N. Ohno, “Dynamic Properties and Discharge Bifurcation of Microwave-sustained Plasma Torch at Atmospheric Pressure”, 2009 Proc. Microwave Discahrges, Fundamentals and Application, CURREAC, Hamamatsu, Japan, September 22-27, pp.65-74.

2) F.M. Dias, J. Henriques, E. Felizardo, E. Tatarova and C.M. Ferreira, “Microwave Plasma Torches driven by Surface Waves”, ibid. pp.101-106.

3) T. Yasui and M. Fukumoto, “Generation of Atmospheric Pressure Microwave Plasma for Plasma Spraying”, ibid. pp.107-112.

4) K. Shinohara, N. Takada and K. Sasaki, “Enhancement of Burning Velocity in Premixed Gas Burner Flame by Irradiating Microwave Power”, ibid. pp.113-117.

5) J. Husarih and M. Kando, “Antenna Excited Microwave Discharge as a Method for Compact Discharge Lamp Operation”, ibid. pp.167-178.

6) T. Okamoto and Y. Okamoto, “High-Power Microwave Induced Helium Plasma at Atmospheric Pressure for Trace Element Analysis”, IEEJ Trans. FM Vol.127, pp.272-276, 2007.

7) H. Yamashita, G. Kushida and T. Takeno, “An Experimental Study on Transition and Mixing Processes in a Coaxial Jet”, Proc. 9th Symp. on Turbulent Shear Flows, Kyoto, Japan, P212-1, 1993.

8) W. Pan, W. Zhang, W. Zhang and C. Wu, “Generation of Long, Laminar Plasma Jets at Atmospheric Pressure and Effects of Flow Turbulence”, Plasma Chem. Plasma Processing, Vol.21, pp.23-35, 2001.

9) S. Takamura, S. Saito, G. Kushida, M. Kando and N. Ohno, “Fluid Mechanical Characteristics of Microwave Discharge Jet Plasmas at Atmospheric Gas Pressure”, IEEJ Trans. FM, Vol.130, pp.493-500, 2010.

10) K. Hayashi, M. Tanaka, H. Yasui and Y. Hashimoto, “Airflow produced by Dielectric Barrier Discharge between Asymmetric Parallel Rod Electrodes”, Rev. Sci Instruments, Vol.78, pp.096103 (3 pages), 2007.

11) M. Moisan, Z. Zakrzewski and J.C. Rostaing, “Waveguide-based Single and Multiple Nozzle Plasma Torches: the TIAGO Concept”, Plasma Sources Sci. Tech., Vol.10, pp.387-394, 2001.

12) S. Takamura, M. Kitoh, T. Soga, H. Takashima, Y. Nishio et al., “Structural Bifurcation of Microwave Helium Plasma Jet Discharge at Atmospheric Pressure”, Plasma Fusion Res., Vol.3, pp.012 (2 pages), 2008.

13) S. Saito, M.A. Razzak, S. Takamura and M.R. Talukder, “Developmant of Asymmetric Double Probe Formula and Its Application for Collisional Plasmas”, J. Applied Phys., Vol.107, pp.123306 (9 pages), 2010.

14) M.A. Razzak, S. Takamura, T. Tsujikawa, H. Shibata and Y. Hatakeyama, “Measurement of Electric Field Distribution along the Plasma Column in Microwave Jet Discharges at Atmospheric Pressure”, Plasma Fusion Res., Vol.4, pp.047 (7 pages), 2009.

15) M.A. Razzak, S. Saito and S. Takamura, “Estimation of Plasma Parameters for Microwave-sustained Ar/He Plasma Jets at Atmospheric Pressure”, Contrib. Plasma Phys., Vol.50, pp.871-877, 2010.

16) M. Tasinsky, J. Mizeraczyk and Z. Zakrzewski, “Stark Broadening in Investigations of Atmospheric-Pressure Microwave Torch Plasmas”, 15th Int. Conf. on Gas Discharges and their Applications GD 2004, Toulouse, France, September 5-10, 2004, pp.817-820.

17) S. Chapman and Cowling, The Mathematical Theory of Non-Uniform Gases, Cambridge University Press, 1952.

18) J.S. Chang, R.M. Hobson, Y. Ichikawa, T. Kaneda, Atomic and Molecular Processes in Ionized Gases, Publication Office, Tokyo Denki University, 1982 (in Japanese).

(受理　平成 23 年 3 月 19 日)